



HAL
open science

SATELLITE-BASED SHORELINE DETECTION FOR MACRO-TIDAL COASTS: IMPACTS OF MORPHOLOGICAL AND HYDRODYNAMIC SETTING

Aikaterini Konstantinou, Timothy Scott, Gerd Masselink, Christopher Stokes,
Daniel Conley, Bruno Castelle

► **To cite this version:**

Aikaterini Konstantinou, Timothy Scott, Gerd Masselink, Christopher Stokes, Daniel Conley, et al.. SATELLITE-BASED SHORELINE DETECTION FOR MACRO-TIDAL COASTS: IMPACTS OF MORPHOLOGICAL AND HYDRODYNAMIC SETTING. Coastal Sediments 2023, Apr 2023, New Orleans, United States. pp.1392-1402, 10.1142/9789811275135_0129 . hal-04266571

HAL Id: hal-04266571

<https://hal.science/hal-04266571>

Submitted on 31 Oct 2023

HAL is a multi-disciplinary open access archive for the deposit and dissemination of scientific research documents, whether they are published or not. The documents may come from teaching and research institutions in France or abroad, or from public or private research centers.

L'archive ouverte pluridisciplinaire **HAL**, est destinée au dépôt et à la diffusion de documents scientifiques de niveau recherche, publiés ou non, émanant des établissements d'enseignement et de recherche français ou étrangers, des laboratoires publics ou privés.

SATELLITE-BASED SHORELINE DETECTION FOR MACRO-TIDAL COASTS: IMPACTS OF MORPHOLOGICAL AND HYDRODYNAMIC SETTING

AIKATERINI KOSNTANTINO¹, TIMOTHY SCOTT¹, GERD MASSELINK¹, CHRISTOPHER STOKES¹, DANIEL CONLEY¹, BRUNO CASTELLE²

1. *Coastal Processes Research Group, School of Biological and Marine Sciences, Plymouth University, UK.*
a.konstantinou@plymouth.ac.uk.
2. *UMR EPOC, CNRS / Université de Bordeaux, Pessac, France.*

Abstract: Robust and accurate long-term mapping of the shoreline is a fundamental requirement for effective coastal management and policy making. Earth observation (EO) coupled with novel image analysis techniques have demonstrated the potential of EO for long-term, local, regional, and even global scale investigations of shoreline change. However, satellite-derived shoreline (SDS) data is associated with large uncertainties relating to environmental factors, tidal range, and wave action among other factors. This contribution investigates the impacts of morphological and hydrodynamic setting on the accuracy of SDS in macrotidal, high-energy coasts. Results revealed significant differences in SDS accuracy between the two morphologically contrasting sites in terms of the level of error and the optimal water level correction. We show that SDS accuracy at macrotidal sites can be greatly improved by applying appropriate water level corrections and that a different approach is required depending on beach type (dissipative/reflective).

Introduction

Robust and accurate long-term mapping of the shoreline is a fundamental requirement for effective coastal management and policy making. However, changes along the shoreline occur over a range of timescales. On one end of the spectrum, intense storm events can result in extreme morphological change within hours on localized scales (e.g., Scott *et al.*, 2015; Harley *et al.*, 2017), whilst at the other end of the spectrum, sea level rise drives coastal evolution at millennial timescales (e.g., Clemmensen *et al.*, 2012). In between, decadal-scale cycles of shoreline change have often been reported, (e.g., Short & Trembanis, 2004; Turner *et al.*, 2016). Interannual and decadal timescales are of particular interest as they are closely linked to modes of global climate variability (e.g., Barnard *et al.*, 2015).

In the North Atlantic, research indicates that the wave climate is strongly linked to large scale atmospheric controls. In particular, Castelle *et al.* (2017) showed that winter-averaged wave conditions in the region can be significantly explained by two climatic indices: the North Atlantic Oscillation (NAO) and the Western Europe Pressure Anomaly (WEPA). Scott *et al.* (2016) noted a consistent decrease in winter-averaged easterly wave power around the Southwest coast of England since the 90's and hypothesized that regional wave forcing was linked to multi-annual atmospheric variability. Recent research demonstrates that winter-averaged inshore wave conditions around the United Kingdom and Ireland, are linked to leading modes of climate variability in the North Atlantic, primarily the NAO, WEPA, and the Atlantic Oscillation (AO) (Scott *et al.*, 2021). Research in the same region has also alluded to the possibility of regionally coherent patterns in coastal response to (Burvingt *et al.*, 2017) and recovery from (Konstantinou *et al.*, 2021) extreme storm seasons. At the same time, a number of studies have attempted to link climate forcing patterns to changes in coastal landform (Scott *et al.*, 2016; Dodet *et al.*, 2019). Burvingt *et al.* (2018), investigated the response of ten sites on the northern coast of SW England over a period of ten years (2007 to 2017) and founded strong connections between winter volume changes observed at the sites and winter averaged WEPA. Wiggins *et al.* (2019b), demonstrated that shoreline alignment in beaches at the south coast of England was largely explained by winter-averaged NAO and WEPA. Concomitantly, other studies have illustrated that NAO is also linked to beach state and nearshore bar dynamics through its control of winter wave conditions (Masselink *et al.*, 2014). Yet to date, our efforts to understand how sandy coasts in the North Atlantic respond to decadal cycles of basin-scale changes have been temporally and spatially limited to a small number of long-term (<16 years) beach monitoring sites.

Optical remote sensing can provide unique and powerful datasets of near global spatial coverage at moderate (10 to 30 m) spatial resolution and regular, short timescales (5 to 15 days), at low to no cost. Novel algorithms have

demonstrated the potential of EO for long-term, local, regional, and even global scale investigations (e.g., Luijendijk *et al.*, 2018; Bishop-Taylor *et al.*, 2021). However, satellite coverage is not uniform across the globe and is further limited in certain areas due to high cloud cover and solar day length amongst other factors. Furthermore, satellite-derived shoreline data is associated with large uncertainties relating to various environmental parameters such as soil moisture, the presence of white water due to wave breaking, sediment type and grain size, and variability in the surrounding terrestrial zone. Tidal range and wave runup present additional challenges for satellite-based applications, particularly at low-gradient sites where small vertical changes in water level can translate to horizontal incursions of the shoreline in the order of hundreds of meters, especially when exposed to high-energy wave climates (Castelle *et al.*, 2021). However, studies assessing the accuracy of satellite-derived shorelines have thus far been largely restricted to microtidal, sandy beaches at lower latitudes. Quantifying and accounting for the effect of these factors on the accuracy of the derived shorelines will increase our confidence in applying EO data to describe shoreline evolution along high-energy, meso-macrotidal coasts. This contribution aims to examine the relationship between physical parameters such as still-water level, wave setup and runup on satellite-derived shorelines, and how this relationship varies with beach type in meso- to macrotidal settings with limited satellite data availability.

Methods

We use CoastSat (Vos *et al.*, 2019b) to extract the shorelines and utilize a 14-year monthly morphological dataset consisting of RTK-GNNS measurements, combined with sea surface elevation and wave model hindcast data (Mercator Ocean 1.5-km reanalysis and UK Met Office 8-km WAVEWATCH III). We focus on two sites representing end members of beach morphological type: Perranporth (Fig. 1a, c) and Slapton Sands (Fig. 1b, d).

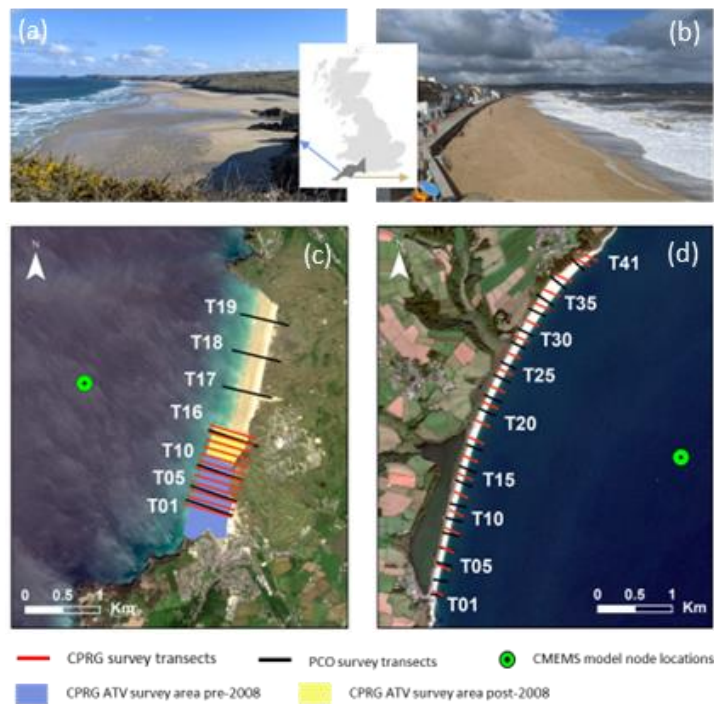


Fig. 1. Overview maps of Perranporth (a) and Slapton Sands (b) and locations of 1D survey profiles and 2D survey areas (Perranporth (c) Slapton (d)). Aerial photos of both sites show the transects along which the survey data was collected. The locations of the wave model nodes are also indicated.

Perranporth beach is a dissipative ($\tan\beta = 0.016$), macrotidal (mean spring tidal range = 6.3 m), sandy embayment ($D_{50} = 0.33\text{--}0.40$ mm) on the north coast of southwest England. The site is fully exposed to a high energy wave climate dominated by prevailing westerly Atlantic storm waves (winter: $H_s = 2.02$ m, $T_p = 12.1$ s; summer: $H_s = 1.22$ m, $T_p = 9.2$ s) (Fig 2a). Slapton Sands is a meso- to macrotidal (mean spring tidal range = 4.4 m), gravel barrier beach ($\tan\beta = 0.13$; $D_{50} = 2.0\text{--}10.0$ mm) on the south coast of southwest England. This site experiences a moderate (winter: $H_s = 0.9$ m, $T_p = 9.1$ s; summer: $H_s = 0.48$ m, $T_p = 7.3$ s), bidirectional wave climate with the main direction from the southwest ($150^\circ\text{--}210^\circ$) and the secondary component from the east ($80^\circ\text{--}130^\circ$) and exhibits typical rotational behavior (Wiggins *et al.*, 2019a) (Fig. 2b,d).

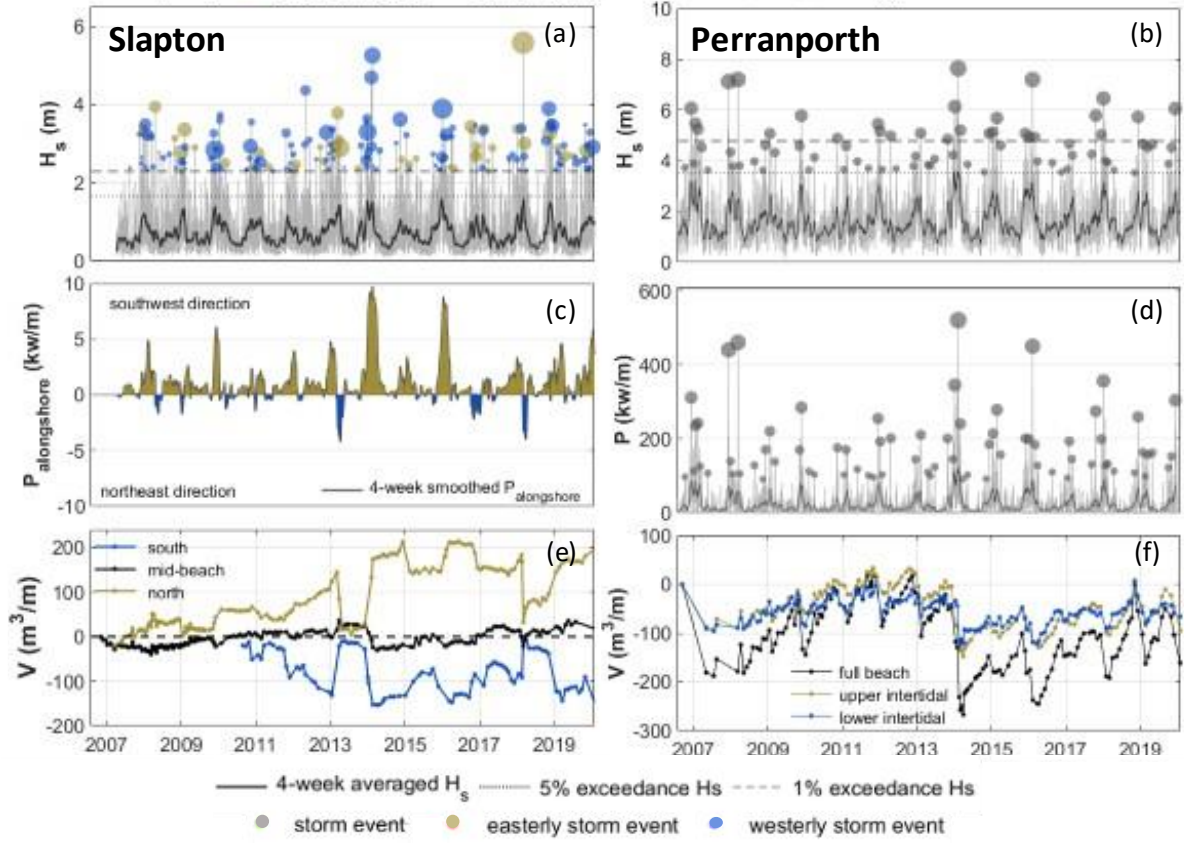


Fig. 2. Wave climate and beach volume time series shown for the two sites. Significant wave height at Slapton (a) and Perranporth (b); alongshore wave power at Slapton (c) and overall wave power at Perranporth (d); beach volume time series for Slapton (e) and Perranporth (f).

We first aim to establish the measurement accuracy of the instantaneous SDS (SDW) and establish the optimum water level parametrization for each site. We test five different water level parametrizations: i) no consideration of water level fluctuations (η_0); ii) including tidal elevation (η_t); iii) including tidal elevation and wave setup (η_{ts}); iv) including tidal elevation and the full Stockdon wave runup (η_{tsr^*}); and v) including tidal elevation and the full Stockdon wave runup after accounting for wave transformation (η_{tsr}).

We calculate wave set up and runup using the equations proposed by (Stockdon *et al.*, 2006):

$$S_{2\%} = 1.1 * 0.35 \tan \beta H_o L_o \quad (1)$$

$$R_{2\%} = S_{2\%} + 1.1 * 0.5 H_o L_o [0.563 (\tan \beta)^2 + 0.004]^{0.5} \quad (2)$$

where L_o , H_o are the deep-water wavelength and height, respectively, H_s is the significant wave height, T_p is the peak period, and $\tan \beta$ is the beach slope. The deep-water wave parameters required in the Stockdon equation were obtained by reverse-shoaling the extracted model data (Stockdon *et al.*, 2006) from the location of the model output nodes to a depth of 1000 m using linear wave theory. To ensure that the derived deep-water wave conditions accounted for the effects of nearshore wave transformation, wave direction and height at breaking were calculated prior to reverse shoaling (Stokes *et al.*, 2021). The breaking wave parameters were calculated using the approach proposed by van Rijn (2014) and Hunt's approximation of wavelength and wave celerity (Hunt, 1979).

We then project the SDW to a relevant reference shoreline to get an equivalent shoreline (SDS) using different methods each requiring different levels of information on beach morphology: i) using a time-invariant transect profile; ii) using a beach-averaged, time-invariant beach slope; iii) using an estimated value for beach slope following Bujan *et al.* (2019).

Results

SDW accuracy

Fig. 3 shows the accuracy of the instantaneous satellite-derived waterlines (SDW) for each water level parametrization tested. Results indicate that including tidal elevation alone led to the highest SDW accuracy at Slapton (RMSE: 14.4 m; mean bias: 7.7 m, seaward) improving RMSE accuracy by 20% and the mean bias by 29%. At Perranporth, including tidal elevation also led to a significant reduction of the RMSE by 78%. However, when considering tidal elevation, the mean bias switched from 16.3 m seaward to 20.3 m landwards, illustrating the possible effect of tidal aliasing. At this site, considering wave-induced water-level fluctuations led to a further considerable reduction of the RMSE by 34% and the mean bias by 78% leading to an overall reduction of 85% in RMSE and 72% in the mean bias. The level of error associated with Perranporth (RMSE = 20.4 m; mean bias = 4.5 m, landward) remained significantly higher than that obtained at Slapton (RMS = 14.4 m; mean bias = 7.7 m, seaward). Interestingly there is a clear difference between the performance of Sentinel 2 (S2) and Landsat 8 (L8) from site to site.

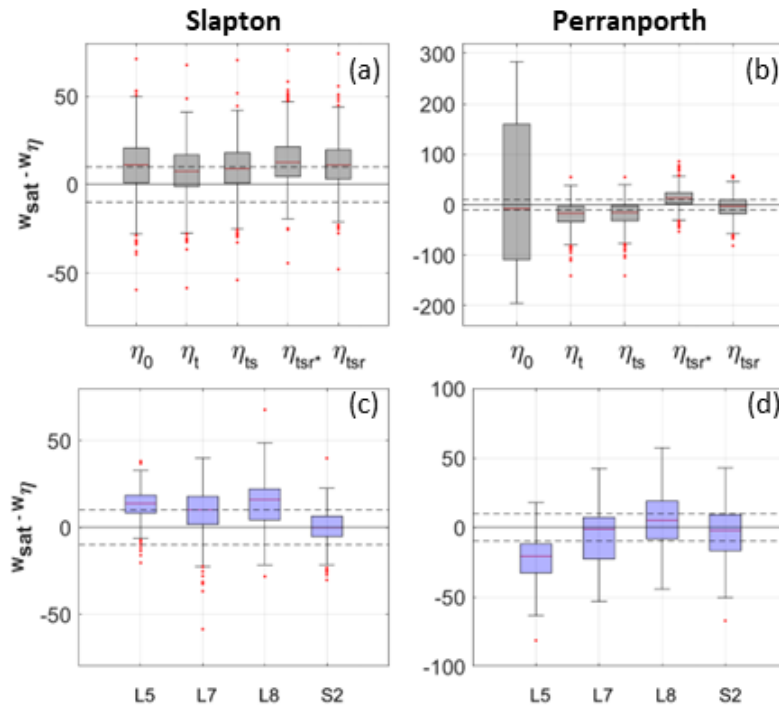


Fig. 3. Top row: SDW error ($W_{sat} - W_{\eta}$) at the two sites derived at every beach profile transect for each image/survey pair up to 30 days apart for the different water level parametrizations (η_0 : no correction; η_t : tidally corrected; η_{ts} : tide and setup; η_{tsr} : tide and full runoff; η_{tsr*} : tide and full runoff after wave transformation). Bottom row: Satellite performance shown for the two sites based on the optimal configuration at each site (Slapton: using η_t ; Perranporth: using η_{tsr}).

SDS accuracy

Further analysis only included the optimal parameterizations at each site based on the results obtain in the previous section, (i.e., η_t for Slapton and η_{tsr} for Perranporth). We examine several methods of translating horizontally a given waterline to some reference shoreline: (i) using a temporally averaged transect profile; (ii) using a mean slope calculated between HAT and LAT, similar to the approach adopted by Vos *et al.* (2019a) and Castle *et al.* (2021) (Slapton: $\tan\beta = 0.125$; Perranporth: $\tan\beta = 0.075$). As both approaches require information on the shape of the beach profile, we also used empirical estimations of beach slope that are more relevant to sites for which no data is available. Consequently, we also translate the SDW to a reference elevation using iii) the empirical relationship proposed by Bujan *et al.* (2019) (Slapton: $\tan\beta = 0.149$; Perranporth: $\tan\beta = 0.075$); and iv) the 25th and 75th quartile beach slope values included in Bujan *et al.* (2019) for gravel and sandy beaches (Slapton: $\tan\beta = 0.09$ and 0.19 respectively; Perranporth: $\tan\beta = 0.02$ and 0.1 respectively). Fig. 4 shows a comparison of SDS RMSE and mean bias for Slapton (for $\eta = \eta_t$) and Perranporth (for $\eta = \eta_{tsr}$) obtained using these different methods to translate the cross-shore locations of the SDW (W_{sat}) to a range of reference shorelines between AMSL and AMSL + 3 m.

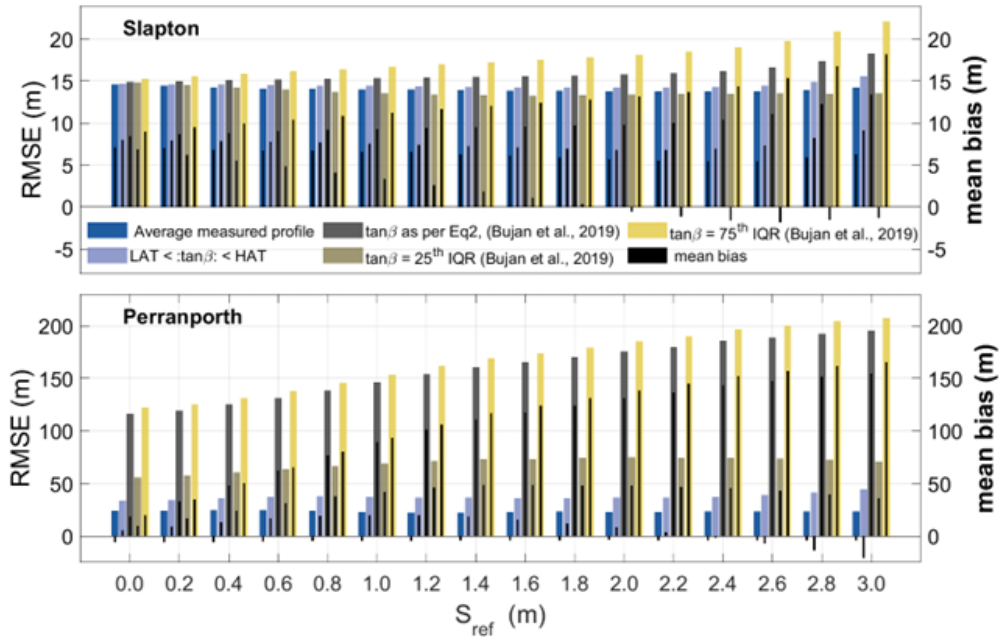


Fig. 4: SDS accuracy achieved with different SDW translation methods at a range of reference shoreline elevations between AMSL and AMSL + 3.0m.

Discussion

This study addressed the influence of tidal elevation and wave-induced water level fluctuations on the accuracy of satellite-derived shoreline data at two different coastal environments in the UK. Results showed that uncertainty in SDS in macro-tidal beach settings can be significantly reduced by defining an appropriate water level parametrization. Further, our results highlighted marked differences in SDS accuracy between the two contrasting sites in terms of the level of error and the optimal water level correction. Results further revealed different, and spatially variable performance between satellite sensors. These findings suggest that the optimal strategy for accurate SDS measurement may be site-specific.

At both sites, accounting for tidal elevation led to a marked reduction in SDW RMSE of 20% at Slapton and 75% at Perranporth. At Perranporth, including the wave runup component was key to achieving a further significant accuracy improvement, reinforcing the findings of Castelle *et al.* (2021). When this correction was applied to the reflective site (Slapton), however, it resulted in reduced accuracy, suggesting that the optimal SDW definition varies with beach type and should be considered in local-scale applications. Nevertheless, η_{tsr} was found to represent the optimal approach for applications that include a variety of different beach types.

In terms of SDS accuracy, the highest accuracy across the board was achieved by using an average measured profile for translating W_{sat} to a reference shoreline. For large-scale applications or when extracting shorelines at sites with little or no information, linear translation using some measure of beach slope is typically the only available option for translating W_{sat} to a reference shoreline. In this case, error was a function of both detection errors and the deviation of beach-face geometry from the theoretical line defined by the translation slope. Consequently, the level of error associated with this method was strikingly higher and greatly influenced the selected shoreline proxy at both sites (Fig. 4).

Conclusion

- Analysis found satellite-derived shoreline accuracy at selected UK sites was significantly improved by applying water level corrections.
- Results indicate a different correction approach is required for water level definition for different beach types (reflective, dissipative).
- Accuracy of SDS depends on chosen proxy shoreline and varies with beach type and shoreline translation method.

Acknowledgements

Our thanks go to all the CPRG members and University of Plymouth students who have been, and still are, contributing their efforts to the CPRG beach survey program. We would also like to thank Kilian Vos and the Water Research Laboratory for developing and making freely available the CoastSat toolkit and for their continuing support.

References

- Barnard, P. L., Short, A. D., Harley, M. D., Splinter, K. D., Vitousek, S., Turner, I. L., Allan, J., Banno, M., Bryan, K. R., Doria, A., Hansen, J. E., Kato, S., Kuriyama, Y., Randall-Goodwin, E., Ruggiero, P., Walker, I. J. & Heathfield, D. K. (2015) 'Coastal vulnerability across the Pacific dominated by El Nino/Southern Oscillation'. *Nature Geoscience*, 8 (10), pp. 801-+. <https://doi.org/10.1038/ngeo2539>.
- Bishop-Taylor, R., Nanson, R., Sagar, S. & Lymburner, L. (2021) 'Mapping Australia's dynamic coastline at mean sea level using three decades of Landsat imagery'. *Remote Sensing of Environment*, 267 pp. 19. <https://doi.org/10.1016/j.rse.2021.112734>.
- Bujan, N., Cox, R. & Masselink, G. (2019) 'From fine sand to boulders: Examining the relationship between beach-face slope and sediment size'. *Marine Geology*, 417 pp. 106012. <https://doi.org/10.1016/j.margeo.2019.106012>.
- Burvingt, O., Masselink, G., Russell, P. & Scott, T. (2017) 'Classification of beach response to extreme storms'. *Geomorphology*, 295 pp. 722-737. <https://doi.org/10.1016/j.geomorph.2017.07.022>.
- Burvingt, O., Masselink, G., Scott, T., Davidson, M. & Russell, P. (2018) 'Climate forcing of regionally-coherent extreme storm impact and recovery on embayed beaches'. *Marine Geology*, 401 pp. 112-128. <https://doi.org/10.1016/j.margeo.2018.04.004>.
- Castelle, B., Dodet, G., Masselink, G. & Scott, T. (2017) 'A new climate index controlling winter wave activity along the Atlantic coast of Europe: The West Europe Pressure Anomaly'. *Geophysical Research Letters*, 44 (3), pp. 1384-1392. <https://doi.org/10.1002/2016gl072379>.
- Castelle, B., Masselink, G., Scott, T., Stokes, C., Konstantinou, A., Marieu, V. & Bujan, S. (2021) 'Satellite-derived shoreline detection at a high-energy meso-macrotidal beach'. *Geomorphology (Amsterdam, Netherlands)*, 383 pp. 107707. <https://doi.org/10.1016/j.geomorph.2021.107707>.
- Clemmensen, L. B., Nielsen, L., Bendixen, M. & Murray, A. (2012) 'Morphology and sedimentary architecture of a beach-ridge system (Anholt, the Kattegat sea): a record of punctuated coastal progradation and sea-level change over the past similar to 1000 years'. *Boreas*, 41 (3), pp. 422-434. <https://doi.org/10.1111/j.1502-3885.2012.00250.x>.
- Dodet, G., Castelle, B., Masselink, G., Scott, T., Davidson, M., Floc'h, F., Jackson, D. & Suanez, S. (2019) 'Beach recovery from extreme storm activity during the 2013–14 winter along the Atlantic coast of Europe'. *Earth Surface Processes and Landforms*, 44 (1), pp. 393-401. <https://doi.org/doi:10.1002/esp.4500>.
- Harley, M. D., Turner, I. L., Kinsela, M. A., Middleton, J. H., Mumford, P. J., Splinter, K. D., Phillips, M. S., Simmons, J. A., Hanslow, D. J. & Short, A. D. (2017) 'Extreme coastal erosion enhanced by anomalous extratropical storm wave direction'. *Scientific Reports*, 7 (1), pp. 6033. <https://doi.org/10.1038/s41598-017-05792-1>.
- Hunt, J. N. (1979) 'Direction solution of wave dispersion equation'. *Journal of Waterway, Port, Coastal, and Ocean Engineering (ASCF)*, 105 (WW4) pp. 457-459.
- Konstantinou, A., Stokes, C., Masselink, G. & Scott, T. (2021) 'The extreme 2013/14 winter storms: Regional patterns in multi-annual beach recovery'. *Geomorphology*, 389 pp. 107828. <https://doi.org/https://doi.org/10.1016/j.geomorph.2021.107828>.

- Luijendijk, A., Hagenars, G., Ranasinghe, R., Baart, F., Donchyts, G. & Aarninkhof, S. (2018) 'The state of the world's beaches'. *Scientific Reports*, 8 (1), pp. 1-11. <https://doi.org/10.1038/s41598-018-28915-8>.
- Masselink, G., Austin, M., Scott, T., Poate, T. & Russell, P. (2014) 'Role of wave forcing, storms and NAO in outer bar dynamics on a high-energy, macro-tidal beach'. *Geomorphology*, 226 pp. 76-93. <https://doi.org/10.1016/j.geomorph.2014.07.025>.
- Scott, T., Masselink, G., O'Hare, T., Saulter, A., Poate, T., Russell, P., Davidson, M. & Conley, D. (2016) 'The extreme 2013/2014 winter storms: Beach recovery along the southwest coast of England'. *Marine Geology*, 382 pp. 224-241. <https://doi.org/10.1016/j.margeo.2016.10.011>.
- Scott, T., McCarroll, R. J., Masselink, G., Castelle, B., Dodet, G., Saulter, A., Scaife, A. A. & Dunstone, N. (2021) 'Role of Atmospheric Indices in Describing Inshore Directional Wave Climate in the United Kingdom and Ireland'. *Earths Future*, 9 (5), <https://doi.org/10.1029/2020ef001625>.
- Scott, T. I. M., Masselink, G., O'Hare, T. I. M., Davidson, M. & Russell, P. (2015) 'Multi-annual sand and gravel beach response to storms in the southwest of England', *Coastal Sediments 2015*. WORLD SCIENTIFIC.
- Short, A. D. & Trembanis, A. C. (2004) 'Decadal Scale Patterns in Beach Oscillation and Rotation Narrabeen Beach, Australia—Time Series, PCA and Wavelet Analysis'. *Journal of Coastal Research*, 20 (2), pp. 523-532. [https://doi.org/10.2112/1551-5036\(2004\)020\[0523:DSPIBO\]2.0.CO;2](https://doi.org/10.2112/1551-5036(2004)020[0523:DSPIBO]2.0.CO;2).
- Stockdon, H. F., Holman, R. A., Howd, P. A. & Sallenger, A. H. (2006) 'Empirical parameterization of setup, swash, and runup'. *Coastal Engineering*, 53 (7), pp. 573-588. <https://doi.org/10.1016/j.coastaleng.2005.12.005>.
- Stokes, K., Poate, T., Masselink, G., King, E., Saulter, A. & Ely, N. (2021) 'Forecasting coastal overtopping at engineered and naturally defended coastlines'. *Coastal engineering (Amsterdam)*, 164 <https://doi.org/10.1016/j.coastaleng.2020.103827>.
- Turner, I. L., Harley, M. D., Short, A. D., Simmons, J. A., Bracs, M. A., Phillips, M. S. & Splinter, K. D. (2016) 'A multi-decade dataset of monthly beach profile surveys and inshore wave forcing at Narrabeen, Australia'. *Scientific Data*, 3 pp. 13. <https://doi.org/10.1038/sdata.2016.24>.
- van Rijn, L. C. (2014) 'A simple general expression for longshore transport of sand, gravel and shingle'. *Coastal Engineering*, 90 pp. 23-39. <https://doi.org/https://doi.org/10.1016/j.coastaleng.2014.04.008>.
- Vos, K., Harley, M. D., Splinter, K. D., Simmons, J. A. & Turner, I. L. (2019a) 'Sub-annual to multi-decadal shoreline variability from publicly available satellite imagery'. *Coastal Engineering*, 150 pp. 160-174. <https://doi.org/10.1016/j.coastaleng.2019.04.004>.
- Vos, K., Splinter, K. D., Harley, M. D., Simmons, J. A. & Turner, I. L. (2019b) 'CoastSat: A Google Earth Engine-enabled Python toolkit to extract shorelines from publicly available satellite imagery'. *Environmental Modelling & Software*, 122 pp. 7. <https://doi.org/10.1016/j.envsoft.2019.104528>.
- Wiggins, M., Scott, T., Masselink, G., Russell, P. & McCarroll, R. J. (2019a) 'Coastal embayment rotation: Response to extreme events and climate control, using full embayment surveys'. *Geomorphology*, 327 pp. 385-403. <https://doi.org/10.1016/j.geomorph.2018.11.014>.
- Wiggins, M., Scott, T., Masselink, G., Russell, P. & Valiente, N. G. (2019b) 'Regionally-Coherent Embayment Rotation: Behavioural Response to Bi-Directional Waves and Atmospheric Forcing'. *Journal of Marine Science and Engineering*, 7 (4), pp. 18. <https://doi.org/10.3390/jmse7040116>.